Wear Analysis of a Ti-5Al-3V-2.5Fe Alloy Using a Factorial Design Approach and Fractal Geometry

Abdel-Wahab El-Morsy
Mechanical Engineering Department
Faculty of Engineering-Rabigh
King Abdulaziz University
Saudi Arabia
Mechanical Engineering Department
Faculty of Engineering-Helwan
Helwan University, Cairo, Egypt
aalmursi@kau.edu.sa

Abstract—**This paper describes the application of the full factorial experimental design technique to confirm the significance of the factors affecting the wear behavior of a recycled Ti-5Al-3V-2.5Fe alloy with a minimum number of experiments. The fractal theory has been used to describe the worn surface state and to investigate the relationship between the fractal dimensions and the surface morphology. The experiments of the sliding wear have been performed under stresses in the range of 1-5 MPa and within sliding velocities range of 0.2–2.0 m/s. Morphology of the worn surfaces investigations has been undertaken using a scanning electron microscope. From the analysis of variance and the nonlinear regression model, the results show that the applied stress has a higher contribution to the wear rate than the sliding velocity.**

Keywords-dry wear; experimental design technique; ti-alloy; fractal geometry technique

I. INTRODUCTION

Titanium alloys are extensively used in critical applications such as biomedical and aerospace applications due to their attractive combination of high strength, low density, and good corrosion resistance [1-2]. For titanium alloys to be used in applications where wear resistance is largely concerned, such as orthopedic prostheses, sufficient wear resistance is required [3]. However, titanium alloys are well known to possess disreputable poor wear property [4-5]. When titanium products are manufactured considerable amounts of machining waste in the form of chips and discards are produced as an outcome. This certainly adds to the already high cost of titanium manufacturing. To add value to titanium manufacturing and reduce the cost, this scrap can be recycled by remelting, whereby some of the titanium is recovered and reutilized in production processes [6-9]. Attention has grown in the wear characterization of titanium alloys in the past decades [10-14]. The rate of material loss or wear rate can be quantified. However, the description of the material deterioration or the wear worn surfaces is generally based upon visual examination.

The wear rate has been recently quantified by utilizing fractal geometry to the micrographic features [15-17]. Fractal geometry theory is finding its application in the wear morphology by characterizing the worn surface with fractal dimensions as the measure of heterogeneity of a set of points on a plane. Fractal geometry is used also to designate complex two or three-dimensional surfaces such as wear worn surfaces. This study explores the wear characteristics of recycled Ti-5Al-3V-2.5Fe alloy machining chips. The full factorial experimental design technique has been used to clarify the influence of the wear parameters, applied stress and sliding velocity on the dry sliding wear of Ti-5Al-3V-2.5Fe alloy. The micrographic images of the wear worn surfaces have been analyzed by fractal geometry using Fourier analysis.

II. EXPERIMENTAL PROCEDURE

The experiments of the dry sliding wear tests have been conducted using titanium specimens containing 5.47% Al, 3.35% V and 2.48% Fe prepared by recycling of the machining chips of a Ti-6Al-4V alloy as part replacement of titanium sponge and expensive alloying elements [9]. The ingots of the Ti-5.5Al-3.5V-2.5Fe alloy have been hot forged with 72.5% total reduction that is started in the β-phase field and finished in the α-β-phase field. Figure 1 shows a schematic of the forging process and the heat treatment sequences.
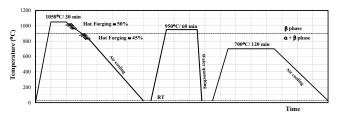

Fig. 1.　Schematic diagram of the hot forging steps and the heat treatment sequence.

The dry sliding wear tests have been performed using wear apparatus, pin-on-ring type [18]. The wear specimens have a diameter of 8 mm and a length of 12 mm. The wear experiments have been conducted in air at room temperature $(25 \pm 2)^{o}$C with dry conditions for a constant sliding distance of 1500 m. Before and after each test, the specimens have been rinsed with acetone and have been dried in air. The wear tests have been conducted under different sliding velocities in the range of 0.2 - 2.0 m/s and applied stresses range of 1- 5 MPa. Weight loss of specimens (ΔW) indicates the wear resistance of the material. ΔW) is computed in the following manner:

$$\Delta W = W_b - W_a \qquad (1)$$

where: W_b = Weight of specimen before test and W_a = Weight of specimen after test. Volumetric wear rate in mm^3/m has been calculated by:

$$WR_v = \frac{\Delta W}{\rho L_s} \qquad (2)$$

where: ρ = density of the material, L_s = Sliding distance .

The experimentation of the dry sliding wear has been conducted with the full factorial experimental design technique by which the number of experiments required, mainly depends on the procedure employed for the design of experiments. The main merit of this technique is to realize the possible interaction between the parameters. In this work, a three-level full factorial design technique has been implemented to analyze the effect of wear parameters, namely, applied stress and sliding velocity, on the volumetric wear rate. The independent parameters and their levels used in this work are listed in Table I. The complete experiment design matrix is summarized in Table II, which shows the experimental combinations of applied stress and sliding velocity.

TABLE I.   INDEPENDENT PARAMETERS AND THEIR LEVELS

Parameters	level			Units
	I	II	III	
Applied Stress, σ	1	3	5	MPa
Sliding Velocity, V	0.2	1.1	2.0	m/s

TABLE II.   EXPERIMENT DESIGN MATRIX

Trail	σ (MPa)	V (m/s)	Wear rate (mm^3/m)
1	1	0.2	0.0206
2	1	1.1	0.0313
3	1	2.0	0.0438
4	3	0.2	0.0404
5	3	1.1	0.1141
6	3	2.0	0.1736
7	5	0.2	0.1026
8	5	1.1	0.1905
9	5	2.0	0.3644

A statistical analysis of variance (ANOVA) has been conducted to recognize the wear parameters and their interactions. Finally, a polynomial model has been developed

for wear rate using regression analysis. The statistical analysis has been conducted using Minitab 17 software. In order to explain the wear behavior, an overall investigation of the worn surfaces of some selected samples has been conducted using the scanning electron microscope (SEM). Worn morphologies have been studied using the image processing and the fractal geometry technique to reveal the effect of independent parameters on the specimen's dry sliding wear.

III.   RESULTS AND DISCUSSION

Figure 2 shows the effect of independent parameters, applied stress and sliding velocity, on the volumetric wear rate. Figure 2(a) shows the wear rate as a function of sliding velocity at constant applied stress. As shown, the wear rates increased with the increasing of the sliding velocity at all the applied stresses. At low applied stress of 1 MPa, the wear rate slightly increased as the sliding velocity increase. As shown, at low applied stress (1 MPa) the line is nearly horizontal and the parameter has a little effect. At 3 MPa applied stress, the wear rates presented a linear increase as a function of sliding velocity. At the highest applied stress of 5 MPa, the wear rate increased linearly until the sliding velocity reached 1.1 m/s. When the sliding velocity surpassed 1.1 m/s, the wear rate abruptly increased as a function of sliding velocity. In addition, the dependence of wear rate on the sliding velocity became marked and the variation is significantly different from the former.
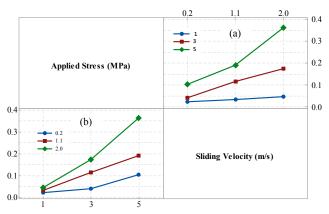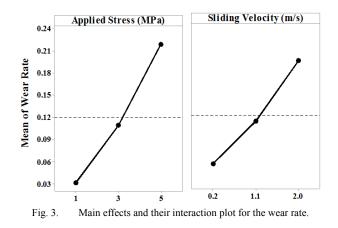

Fig. 2.   Interaction plot for wear rate, (a) effect of sliding velocity and (b) effect of stress.

The influence of the applied stress on the wear rate at constant sliding velocity is shown in Figure 2(b)**.** The wear rate-applied stress relationship under varying sliding velocity exhibits that the wear rate increased linearly and rapidly as a function of applied stress until the highest applied stress. As the sliding velocity increased, the slope of the wear rate increased.

The main effects plot for sliding parameters affecting the wear rate for the mean value is shown in Figure 3. The highest point for each parameter shows the best level. As shown, the applied stress has higher inclination than the sliding velocity. From the inclination of the graph, the contribution of the applied stress on the output response, volumetric wear rate, is stronger than that of the sliding velocity. It is reported that a

parameter with the greater effect on the line has the highest inclination [12]. The relationship between the wear parameters, sliding velocity, V, and applied stress, σ and the output response, volumetric wear rate is obtained by nonlinear regression analysis. Finally, the following polynomial model is fitted to the volumetric wear rate. From this model, it is confirmed that the most influencing parameter is the applied stress compared to the sliding velocity. The value of the determination coefficient, $R^2 = 0.997$, for the wear behavior designates that less than 1% of the variance is not explicated, which indicates the high significance of the model.

$$WR_v = 0.042 - 0.0318\,(\sigma) - 0.0862\,(V) + 0.115(\sigma \times V)$$
$$+ 0.0081\,(\sigma^2) + 0.0328\,(V^2) + 0.0089(\sigma^2 \times V^2)$$
$$- 0.0184\,(\sigma^2 \times V) - 0.0406(\sigma \times V^2)$$
$$+ 0.00014(\sigma\,3) - 0.00001(\sigma\,4) \qquad (3)$$

Fig. 3.   Main effects and their interaction plot for the wear rate.

The significance of the model has been tested using 3D contour map (quadratic presentation) and the analysis of variance (ANOVA) technique. Figure 4 presents the interaction of the two-wear parameter for the response value of the volumetric wear rate using the polynomial model. To elucidate the previous relationship, the effect of each wear parameter on the wear rate has been reconstructed in the form of a contour map. The optimum combination of the wear parameters to enhance the response wear rate can be easily assessed from this figure. The sliding velocity, the applied stress, and the volumetric wear rate are considered as three perpendicular axes. The means of the normal probability plot of the residuals (the difference between the experimental values and the predicted values) has been used to evaluate the normality of the wear rate data as shown in Figure 5. The normal probability plot reveals that the residuals points are very close to a straight line. This means the errors are negligible. The points randomly scattered in residual versus the fitted value graph determine that errors are negligible having constant variance. The relationship between the residuals and the observation order for a volumetric wear rate has been plotted to verify the independence of the wear data. The plot confirms that there is no expectable pattern observed because all the residues lay between the levels. These results are sufficient to show the adequacy of the polynomial model shown in (3). Table III

shows the analysis of variance with the wear parameters percentage contribution. The applied load percentage (55.66 %) is the main controlling parameter on the volumetric wear behavior. In the case of interaction (12.88 %), they have less contribution in the output response.
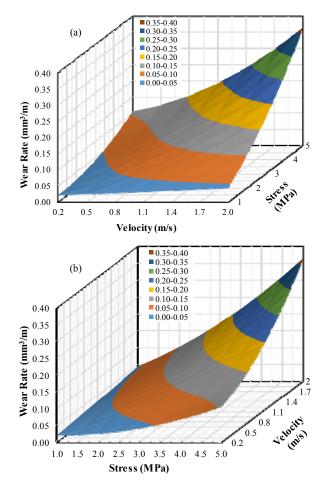

Fig. 4.   Contour surface of wear rate as a function of applied stress and sliding velocity.

Figure 6 shows the worn surface morphology after dry sliding wear at different wear conditions (different applied stresses and sliding velocities). It can be found from the series of images shown that many adhesive traces, grooves, debris, and ploughing marks are evident on all the worn surfaces. Such topographies are features of abrasion causing wear by the removal of small fragments. The wear rate in the segmented area increases steadily as the wear parameters increases. Once the applied stress is above 3 MPa, a sudden increase in the wear rate is notified. Figure 6(f) shows the severely of wear rate on the worn surface tried at 5 MPa applied stress and 2.0 m/s sliding velocity. The SEM micrograph images of the worn surfaces features in the grayscale at a magnification of X200 (scan area 622×416 μm^2) shown in Figure 6 have been analyzed using the image processing and the fractal geometry technique based on Fourier analysis and are shown in Figure 7. The fitting curve has been applied to the data attained to

interpret and correlate an evident linear relationship between log magnitude and log frequency. Then the fractal dimension of all the samples has been calculated. The fractal values which can indicate the degree of complexity of the worn surface are varying between 2.06 at low independent wear parameters and 2.87 at high independent wear parameters. Low fractal values indicate regularity surfaces and high fractal values indicate highly irregular surfaces. It can be found from the series of worn surfaces (the intensities of the grayscale image) shown in Figure 7 that the segmented area (white pixel areas) increases steadily as the applied stress increases. Once the applied stress is above 3 MPa, a rapid increase in the segmented area is notified.
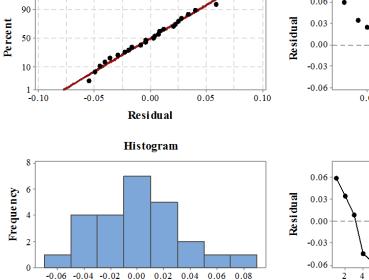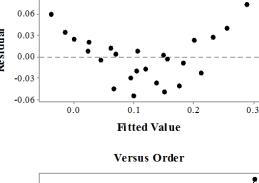
TABLE III.   ANALYSIS OF VARIANCE WITH THE PARAMETERS CONTRIBUTION

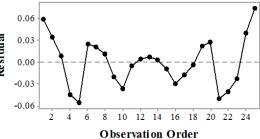| Source	DF	Adj SS	Adj MS	Contribution
Stress	4	0.06377	0.015943	31.16 %
Velocity	4	0.11390	0.028475	55.66 %
Velocity*Stress	16	0.026356	0.001686	12.88 %
Error	2	0.000614	0.000038	0.3 %
Total	26	0.20465		100 %

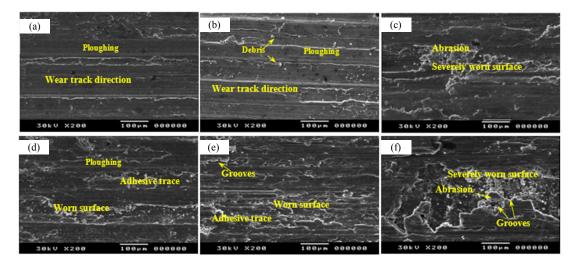Fig. 5.   The residual plots for the volumetric wear rate

Fig. 6.   SEM micrographs of the worn surfaces: (a) 0.2 m/s - 1 MPa, (b) 0.2 m/s – 3 MPa, (c) 0.2 m/s – 5 MPa, (d) 2.0 m/s - 1 MPa, (e) 2.0 m/s – 3 MPa, and (f) 2.0 m/s – 5 MPa.

It is stated that the magnification can affect the physical interpretation regarding the structures and distributions of the worn surfaces [19]. Therefore, the fractal values of the SEM images of the wear samples under different magnifications, high magnification of X500 (scan area 229×171.5 μm^2) and low magnification of X200 (scan area 622×416 μm^2) have been analyzed to quantify the variations in the fractal dimensions. The fractal values of the wear samples under different

magnifications are shown in Figure 8. The figure demonstrates that the fractal dimension of the samples increases gradually with an increase of magnification ratios. Under high magnification, the worn surface has higher fractal dimension compared with the value of low magnification. The samples at high applied load (5 MPa) have the highest fractal dimension values both under high magnification and under low magnification.
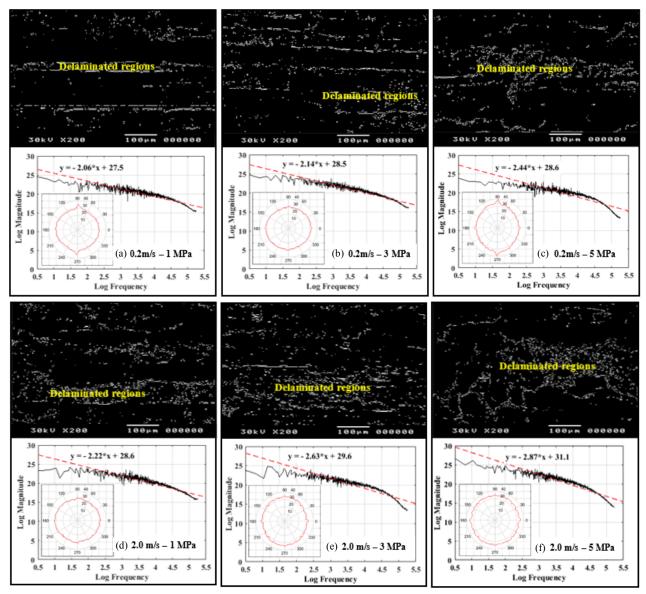

Fig. 7.   Analysis of worn surface using the image processing and the fractal geometry theory.

IV.   CONCLUSIONS

The wear behavior of the recycled Ti-5Al-3V-2.5Fe machining chips sliding against stainless steel counterfaces has been investigated and interpreted. The experimentation of the dry wear tests has been conducted by the full factorial experimental design technique.

The main findings are summarized as follows:

- The relationship between the wear parameters, sliding velocity and applied stress, and the output response, volumetric wear rate is obtained by nonlinear regression analysis. The value of the determination coefficient of the polynomial model (R2 = 0.997) for the wear behavior

indicates that less than 1% of the variance is not explicated, which indicates the high significance of the model.

- It is clear from the analysis of variance that the applied stress has higher inclination than the sliding velocity. From the inclination of the graph, the contribution of the applied stress on the wear rate is stronger than that of the sliding velocity.

- The SEM image processing and fractal dimensions of the worn surfaces have been investigated for the purpose of wear monitoring. The results showed that the procedures are influential techniques since they are effective in characterizing the changes in the surface morphology. Fractal dimension considers the difference in grayscale within a given scan area on different scales.

- The results of the fractal dimension also exhibited that under high magnification, the worn surfaces had a higher fractal dimension (2.29-2.89) than the worn surfaces under the low magnification (2.06-2.87), which corresponded to higher complexity in the worn surface due to the existence of more such areas in the image.
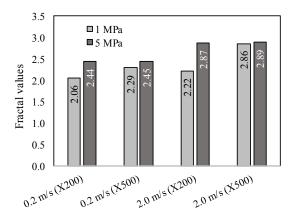

Fig. 8.   Fractal values of the worn surfaces under different magnifications.

REFERENCES

[1]   I. Gurrappa, "Characterization of titanium alloy Ti-6Al-4V for chemical, marine and industrial applications", Materials Characterization Vol. 51, No. 2-3, pp. 131-139, 2003

[2]   I. V. Gorynin, "Titanium alloys for marine application", Materials Science and Engineering: A, Vol. 263, No. 2, pp. 112-116, 1999

[3]   J. Bauer, S. Cella, M. Pinto, J. Costa, A. Reis, A. Loguercio, "The use of recycled metal in dentistry: Evaluation of mechanical properties of titanium waste recasting", Resources, Conservation and Recycling, Vol. 54, No. 12, pp. 1312-1316, 2010

[4]   P. Jiang, X. He, X. Li, L. Yu, H. Wang, "Wear resistance of a laser surface alloyed Ti-6Al-4V alloy", Surface and Coatings Technology, Vol. 130, No. 1, pp. 24-28, 2000

[5]   C. Martini, L. Ceschini, "A comparative study of the tribological behaviour of PVD coatings on the Ti-6Al-4V alloy", Tribology International Vol. 44, No. 3, pp. 297-308, 2011

[6]   P. Veronesi, S. Gaiani, E. Colombini, G. Poli, R. Tisu, "Recycling of alpha-titanium technological scrap for exhaust system parts manufacturing", Journal of Cleaner Production Vol. 53, pp. 332-340, 2013

[7]   P. Luo, D. McDonald, S. Zhu, S. Palanisamy, M. Dargusch, K. Xia, "Analysis of microstructure and strengthening in pure titanium recycled from machining chips by equal channel angular pressing using electron backscatter diffraction", Materials Science and Engineering: A, Vol. 538, pp. 252-258, 2012

[8]   P. Luo, D. McDonald, S. Palanisamy, M. Dargusch, K. Xia, "Ultrafine-grained pure Ti recycled by equal channel angular pressing with high strength and good ductility", Journal of Materials Processing Technology, Vol. 213, No. 3, pp. 469-476, 2013.

[9]   A. El-Morsy, "Microstructural characterization of Ti-6Al-4V machining chips after remelting and bulk hot deformation", Materials & Design, Vol. 30, No. 5, pp. 1825-1829, 2009

[10] H. Attar, K. Prashanth, A. Chaubey, M. Calin, L. Zhang, S. Scudino, J. Eckert, "Comparison of wear properties of commercially pure titanium prepared by selective laser melting and casting processes", Materials Letters, Vol. 142, pp. 38-41, 2015

[11] Q. Wang, P. Zhang, D. Wei, X. Chen, R. Wang, H. Wang, K. Feng, "Microstructure and sliding wear behavior of pure titanium surface modified by double-glow plasma surface alloying with Nb", Materials & Design, Vol. 52, pp. 265-273, 2013

[12] K. Chen, Y. Zhou, X. Li, Q. Zhang, L. Wang, S. Wang, "Investigation on wear characteristics of a titanium alloy/steel tribo-pair", Materials & Design, Vol. 65, pp. 65-73, 2015

[13] L. Mohan, C. Anandan, "Wear and corrosion behavior of oxygen implanted biomedical titanium alloy Ti-13Nb-13Zr", Applied Surface Science, Vol. 282, pp. 281-290, 2013

[14] B. Ganesh, W. Sha, N. Ramanaiah, A. Krishnaiah, "Effect of shot peening on sliding wear and tensile behavior of titanium implant alloys", Materials & Design, Vol. 56, pp. 480-486, 2014

[15] Y. Shen, X. Liu, X. Yuan, "Fractal Dimension of Irregular Region of Interest Application to Corn Phenology Characterization", IEEE Journal of Selected Topics in Applied Earth Observations and Remote Sensing, Vol. 10, No. 4, pp. 1402-1412, 2017

[16] L. Ribeiro, A. Horovistiz, G. Jesuino, L. Hein, N. Abbade, S. Crnkovic, "Fractal analysis of eroded surfaces by digital image processing", Materials Letters, Vol. 56, No. 4, pp. 512-517, 2002

[17] C. Yuan, J. Li, X. Yan, Z. Peng, "The use of the fractal description to characterize engineering surfaces and wear particles", Wear, Vol. 255, No. 1-6, pp. 315-326, 2003

[18] A. W. El-Morsy, "Dry sliding wear behavior of hot deformed magnesium AZ61 alloy as influenced by the sliding conditions", Materials Science and Engineering: A, Vol. 473, No. 1-2, pp. 330-335, 2008

[19] K. Liu, M. Ostadhassan, "Multi-scale fractal analysis of pores in shale rocks", Journal of Applied Geophysics, Vol. 140, pp. 1-10, 2017